Available online at www.sciencedirect.com
SCIENCE DIRECT®
Polymer 45 (2004) 927–935
polymer
www.elsevier.com/locate/polymer

Hard segment connectivity in low molecular weight model 'trisegment' polyurethanes based on monols

Ashish Aneja, Garth L. Wilkes*

Polymer Materials and Interfaces Laboratory, Department of Chemical Engineering, Virginia Polytechnic Institute and State University, Blacksburg, VA 24061-0211, USA

Received 30 June 2003; received in revised form 10 November 2003; accepted 12 November 2003

Abstract

Low molecular weight model trisegmented polyurethanes based on monofunctional polyols, or 'monols', with water-extended toluene diisocyanate (TDI) based hard segments (HS) are investigated. The formulations of the materials generated are similar to those of flexible polyurethane foams with the exceptions that the conventional polyol is substituted by an oligomeric monofunctional polyether of ca. 1000 g/mol molecular weight; and no surfactant is utilized. Plaques formed from these model systems are shown to be solid materials at ambient even at their relatively low molecular weights of 3000 g/mol and less. SAXS, DSC, and AFM are utilized to investigate the microphase separated morphologies of the samples generated. WAXS results show that the local packing of the HS is of a similar nature as that in actual flexible polyurethane foams. AFM phase images, for the first time, reveal the ability of the HS to self-assemble through bidentate hydrogen bonding and form lath-like percolated structures, resulting in solid plaques, even though the overall volume of the system is well dominated by the two terminal liquid-like polyether segments.

Keywords: Polyurethanes; Block copolymers; Microphase separation

1. Introduction

Introduced by Bayer [1,2] in the 1940s, polyurethanes (hereafter abbreviated as PU), stimulated considerable interest during the last five or so decades due to their technologically important as well as interesting structure-property behavior caused by the formation of a microphase separated morphology. The early work of Schollenberger [3,4] and Cooper and Tobolsky [5] established that segmented PUs consist of high T_g or high T_m 'hard' domains microphase-separated from relatively low T_g 'soft' domains. The properties of these materials can be tailored by adjusting the molecular weight, chemistry, topology, and composition of the different segments to promote materials ranging from soft elastomers to rigid, hard thermoplastics [6]. The applications of PUs are principally in the area of foams, elastomers, adhesives, sealants and coatings with a production of approximately 8.2 million metric tons worldwide [7].

The dominant application of PUs is in flexible foams which are utilized in transportation, furniture, and packaging applications [8]. The preparation of these foams involves two simultaneously occurring reactions. One of the reactions, between a diisocyanate and water, generates urea based hard segments (HS) and also produces carbon dioxide which helps in foam expansion. In the other reaction, isocyanate groups also react with the hydroxyl groups of a polyol (functionality >2) to form a chemical network as promoted by the urethane linkages which covalently bond the HS to the soft segments (SS). In the midst of these reactions, microphase separation of the HS into bidentate hydrogen bonded urea microdomains occurs when the product of the degree of polymerization (N) and the interaction parameter (χ) increase to the extent that thermodynamic boundaries are surpassed [9]. The presence of a microphase separated morphology in flexible PU foams was first demonstrated using SAXS by Wilkes and co-workers [10]. It is often viewed that since the percentage of polyol is typically greater than that of the urea microdomains, the polyol is the continuous phase in which the microdomains are dispersed [8,10]. In addition, workers

* Corresponding author. Tel.: +1-540-231-5498; fax: +1-540-231-9511.
E-mail address: gwilkes@vt.edu (G.L. Wilkes).

0032-3861/$ - see front matter © 2003 Elsevier Ltd. All rights reserved.
doi:10.1016/j.polymer.2003.11.038

have also shown that for the common 'slabstock' PU foams, large scale aggregation of the urea microdomains can take place leading to the formation of regions rich in urea which are referred to as urea 'balls' or urea 'aggregates' [11,12]. This aggregation behavior was first reported in a study carried out by Armistead et al. who reported ca. 300 nm sized urea aggregates, using TEM, for the slabstock foam formulation which they investigated [11]. Recent efforts by Ade et al. [12] and Rightor et al. [13] have further confirmed and elucidated the structure and composition of the urea aggregates and these workers have shown that the aggregates are not purely based on urea HS but also have some polyol residing within them.

Most commercial PU foams in North America utilize the 80:20 2,4/2,6 toluene diisocyanate (TDI) mixture and polyether polyols which are based on ethylene oxide (EO), or propylene oxide (PO), or both kinds of repeating units [8]. The EO vs PO content, EO end-capping reactivity characteristics, and molecular weight of the polyol are adjusted according to the type of process used to prepare the foam. Slabstock foams, which are prepared in a semi-continuous manner, generally utilize trifunctional glycerin-extended polyols with a molecular weight of ca. 3000 g/mol as opposed to ca. 5000 g/mol for the batchwise molded foam process. This is because molded foams require a faster viscosity build up which is necessary to ensure shorter demold times. For the same reason, molded foam polyols also have higher EO contents and are also usually EO end-capped.

The issue of HS connectivity and its implications on the physical properties of linear PU elastomers has been addressed [14]. On analyzing a series of PU elastomers, containing 15, 25, 35, and 45 wt% HS, Abouzahr and Wilkes suggested that at HS contents greater than ca. 25 wt%, an interlocking hard domain morphology was developed. Their argument was based primarily on data obtained using X-ray scattering (SAXS, WAXS) and mechanical property measurements. They noted that the material containing 25 wt% HS displayed good elastomeric properties (high extensibility/recovery, low hysteresis) and suggested that the hard domains in this material were relatively isolated. On increasing the HS content to 35 and 45 wt% it was observed that the interlocking hard domain texture of these materials promoted higher moduli. They also proposed that due to the presence of a more continuous hard phase, these materials showed low extensibility and behaved more like rigid thermoplastics. However, no direct *visual* representation using any microscopy techniques of their suggested morphologies was provided at that point. Seymour and Cooper have also proposed interconnecting hard domain morphologies on analyzing the orientation elongation behavior of PU elastomers [15].

Recent research in the area of PU foams carried out in our laboratory has suggested that the connectivity of the urea HS can play an important role in determining the physical properties of flexible PU foams. Work in our group has focused on investigating urea phase connectivity in flexible PU foam formulations using lithium salts as additives to disrupt the association of the urea phase at different scale lengths [16–19]. From this work, it has been shown that mechanical and viscoelastic properties change as a result of altering the association of the urea phase. The experimental work has also been supported by quantum mechanical simulations (using density functional theory) performed on model compounds possessing functional groups/linkages found within PU foams [18,19].

Elwell and co-workers investigated the in situ development of flexible PU foam morphology under forced adiabatic conditions [20]. They studied MDI based foams with a water content of 2.2 pphp and studied systems in which either a conventional polyether polyol (functionality >2), or a monofunctional polyol (monol) was used as a SS. They found that microphase separation occurred at approximately the same isocyanate conversion for both the monol and polyol foams. Using synchrotron SAXS the workers showed that the interdomain spacings for the monol and polyol foams were ca. 100 Å and remained unchanged during as the structure developed for either system. The workers also concluded that the presence of covalent cross-links in the polyol foam delayed the onset of microphase separation of the urea HS.

The present study will utilize monols with molecular weights of ca. 1000 g/mol, i.e. essentially one arm of a conventional polyether polyol. By doing so, the covalent cross-linking points which are otherwise present in typical triol containing foams are eliminated as is the development of any high molecular weight polymer. The emphasis in this study shall be on the morphological structure developed in these model 'trisegment' systems. The first ever visual representation of the extent of HS connectivity, as promoted by strong bidentate hydrogen bonding, in these unique systems will also be provided via AFM.

2. Experimental

2.1. Materials

The present study makes use of several samples which were prepared at Dow Chemical, Freeport, TX. The isocyanate used was an 80:20 mixture of the 2,4 and 2,6 toluene diisocyanate isomers, and was added to stoichiometrically react with the water and/or monol. Deionized water was used as the chain extender. Two series of materials were investigated based on different monols, both of which have a molecular weight of 1000 g/mol and functionality = 1. One monol was a heterofed ethylene oxide (EO) and propylene oxide (PO) random copolymer with an EO content of 50 wt%. The other monol was purely based on PO repeat units. These monols are referred to as EP-Monol and PP-Monol, respectively (Table 1). It is also pointed out that the conventional nomenclature scheme of 'parts per hundred

Table 1
Sample designations and their meanings

Sample ID	Comments	Wt% HS
EP-Monol	Heterofed 50:50 EO/PO monol	–
EP-TDI-EP	Trisegment with a single TDI unit between two EP-Monol chains	–
EP-1.0W-EP	Trisegment with a 1.0 water pphp and TDI based HS and two EP-Monol SS	15.9
EP-1.5W-EP	Trisegment with a 1.5 water pphp and TDI based HS and two EP-Monol SS	18.8
EP-2.0W-EP	Trisegment with a 2.0 water pphp and TDI based HS and two EP-Monol SS	21.5
EP-4.0W-EP	Trisegment with a 4.0 water pphp and TDI based HS and two EP-Monol SS	30.6
EP-6.0W-EP	Trisegment with a 6.0 water pphp and TDI based HS and two EP-Monol SS	37.8
PP-1.0W-PP	Trisegment with a 1.0 water pphp and TDI based HS and two PP-Monol SS	15.9
PP-1.5W-PP	Trisegment with a 1.5 water pphp and TDI based HS and two PP-Monol SS	18.8
PP-2.0W-PP	Trisegment with a 2.0 water pphp and TDI based HS and two PP-Monol SS	21.5
PP-4.0W-PP	Trisegment with a 4.0 water pphp and TDI based HS and two PP-Monol SS	30.6
PP-6.0W-PP	Trisegment with a 6.0 water pphp and TDI based HS and two PP-Monol SS	37.8

Note: HS—hard segment, SS—soft segment, EO—ethylene oxide, PO—propylene oxide, TDI—80:20 2,4/2,6 toluene diisocyanate.

polyol (pphp)' will be used in this article, irrespective of the fact that the 'polyol' in the present study is actually a monol. A conventional catalyst package, where utilized, was added at 0.2 pphp, and consisted of 5 parts by weight of Dabco 33LV for each part of Dabco BL11. Specific details regarding the catalysts can be found elsewhere [8]. As discussed later, since the materials made were plaques and films and not actual foams, there was no desire to form a stable cellular structure, and hence no surfactants were utilized.

2.2. Preparation of EP-TDI-EP and PP-TDI-PP

The monols were used to prepare several 'trisegmented' species. In one case, the monols were reacted with a stoichiometric amount of TDI to form a material which contained two monol SS separated from each other by a single TDI unit (Fig. 1(a)). This material possesses only urethane linkages but no urea groups (since no water is used). No catalysts were added in these two formulations, referred to as EP-TDI-EP and PP-TDI-PP (Table 1).

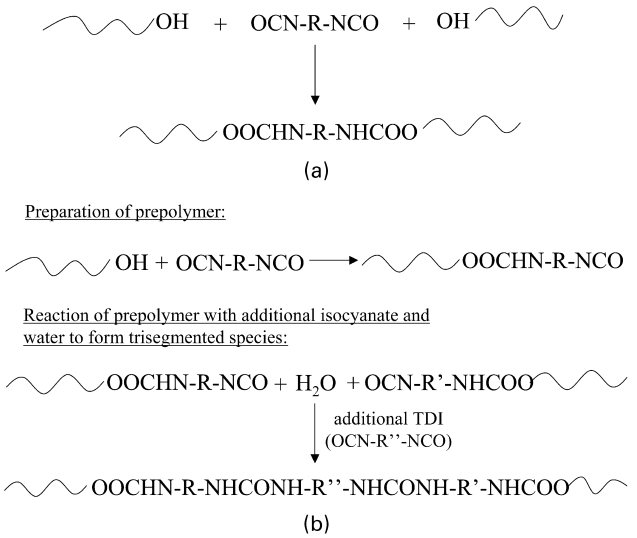

Fig. 1. (a) Reaction scheme for preparation of PP-TDI-PP and EP-TDI-EP. (b) Reaction scheme for preparation of trisegmented species with water and TDI based hard segments and monol soft segments.

2.3. Preparation of films cast from reacting mixtures

Several films (ca. 50 μm thick), based on EP-Monol and PP-Monol, in which water was reacted with TDI to form HS were also prepared. Table 1 presents the nomenclature scheme used. For example, EP-2.0W-EP contains two EP-Monol SS. the designation of '2.0W' for this formulation indicates that HS in this sample are based on the reaction of 2.0 water pphp and TDI. The weight percentages of HS for these samples range from 15.9 to 37.8 wt% and are listed in Table 1.

The preparation of the films was carried out by the 'prepolymer' method. Two equivalent weights of the isocyanate were added to the monol at room temperature while stirring. Stirring of the prepolymer was continued at 1500 rpm for ca. 50 s followed by placing it in an oven at 60 °C for 24 h. The prepolymer, water, and catalyst were added in a 400 ml beaker and mixed for 50 s at 2000 rpm using a 1′ diameter stirring paddle. Additional isocyanate was also introduced in the mixture and stirring was continued for a total stirring time of 100 s. The chemical reactions are outlined in Fig. 1(b). As stated earlier no surfactant was included in the formulation. Stirring was continued until CO_2 evolution ceased. At this point, a small amount of the reacting mixture (ca. 50 mg) was removed and placed on a clean glass slide. A doctor blade was then used to cast a ca. 50 μm film. The glass slide was then placed in an oven operating at 100 °C for 1 h, followed by 24 h at 60 °C, in order to facilitate completion of the reactions.

It is essential to point out that in the prepolymer technique outlined above, the formation of some trisegmented species in which the same TDI molecule reacted

with two monol chains could *not* be precluded. Simple probability calculations show that the amount of trisegmented species in which the same TDI molecule reacts at both NCO positions with monol chains would be 25%. However, the percentage of such species in our system would be distinctly less than 25%, due to the known relative reactivities of the isocyanate groups on 2,4 and 2,6 TDI [8]. For the 2,4 isomer, it is known that the reactivity of the ortho position in the 2,4 isomer is approximately 12% of the reactivity of the isocyanate group in the para position. For this reason, there would be only very few 2,4 TDI molecules which would react at *both* ends during the preparation of the *prepolymer*. For 2,6 TDI, the isocyanate groups have equal reactivities when both groups are unreacted. However, after one of the isocyanate groups reacts, the reactivity of the second group drops by a factor of ca. 3, thereby reducing the probability of 2,6 TDI molecules reacting at *both* isocyanate sites during the synthesis of its prepolymer.

2.4. Preparation of plaques

The procedure for preparation of the plaques was the same as that used for making the above films, with one difference in the final step. Instead of casting a film, the reacting mixture was taken and quickly poured on Teflon sheets supported by steel plates and placed in a hot-press operating at 100 °C and 20,000 lb_f for 1 h. A picture-frame mold ca. 0.05′ thick was utilized. At the end of 1 h, the plaque was removed and allowed to cool at ambient conditions.

2.5. Preparation of films cast from solution

To compare and reinforce the morphological observations noted in the films cast from the reacting mixture, solution cast films were also prepared. These films were cast by making a ca. 10 wt% solution of the plaque counterpart using DMAc as the solvent. A small amount of the solution was then placed on a clean glass slide and a film was cast using a doctor blade. The slide was then placed in an oven at 60 °C for 2 h and subsequently under vacuum for 24 h to ensure complete removal of the solvent.

2.6. Methods

SAXS, WAXS, FTIR, DSC, and AFM were utilized to characterize the above materials. SAXS and AFM were used to give insight into the microphase separation behavior where as WAXS was employed to study the intersegmental ordering of the HS at the 1–10 Å length scale. The SS glass transition behavior was probed using DSC. These techniques have been extensively utilized by the authors to study PU plaques and foams and the experimental details associated with these methods can be found elsewhere [16,17].

3. Results and discussion

Since a large number of samples were prepared in order to carry out this study, it will not be possible to utilize the results for all the samples investigated. Instead, selected results, which are representative of this study are presented.

Fig. 2 shows a photograph of plaque EP-2.0W-EP, which contains ca. 22 wt% HS. Recall that this material principally contains trisegments based on two EP-monol chains, and HS which are formed by the reaction of TDI and 2.0 water pphp. Molecular weight build up is limited to trisegments for this and other similar materials since a monol can react only at one position. This means that the overall average molecular weight for such trisegment species is always less than 3000 g/mol, which is much lower than the molecular weight for entanglements. Interestingly, even at such a low molecular weight, this material is a distinct solid, as seen in Fig. 2. Clearly, the hydrogen bonding capabilities of the urea and urethane moieties are playing a significant role in promoting the percolation of the HS phase and thus the solidification of these plaques. Also, it is suggested that the hydrogen bonding interactions are not only local within hard domains, but promote long range effects leading to the build-up of an interconnected HS network. In other words, the ability of the HS to self assemble and ‘connect’ with each other is absolutely required to achieve solidification of these materials. Further proof of this hypothesis will be presented later in this article using AFM. The solidification of *non*-polymeric species of cholesteryl 4-(2-anthryloxy)-butanoate (CAB)/hexadecane and CAB/dodecane gelators, via the formation of three-dimensional interlocking morphologies based on weak attractive intermolecular interactions (dipolar and van der Waals forces), has also been demonstrated by Lin et al. [21].

Fig. 3 presents selected SAXS results obtained for the

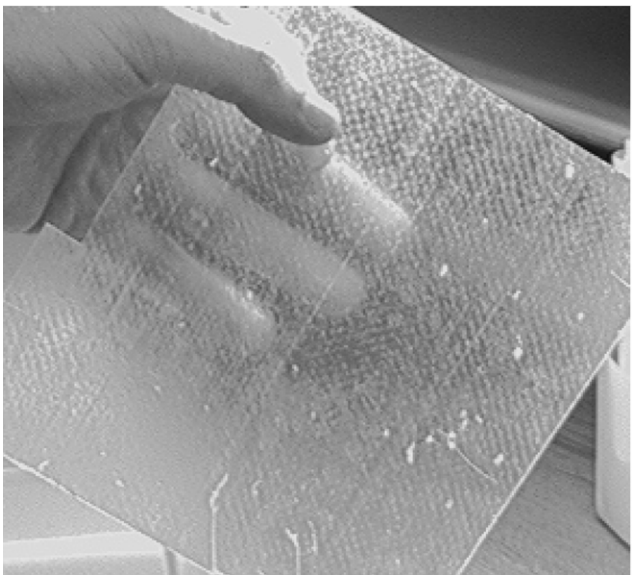

Fig. 2. Photograph of EP-2.0W-EP showing its solid state.

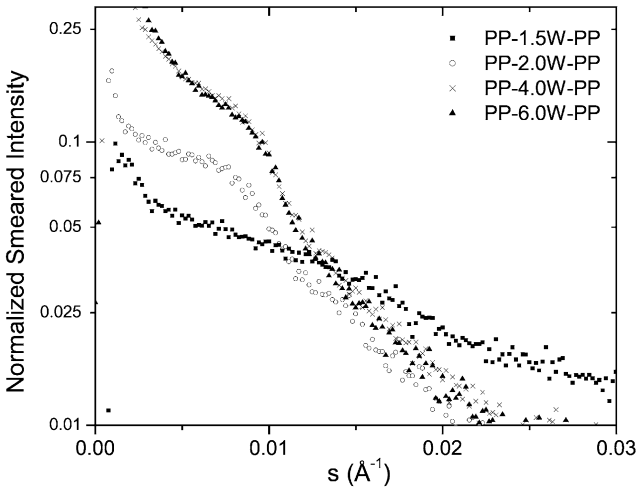

Fig. 3. Small angle X-ray scattering profiles as a function of water (hard segment) content for plaques based on PP-Monol soft segment.

plaques which utilized PP-Monol as the SS and contain varied HS levels. The ordinate and abscissa display log(normalized 'smeared' scattered intensity) and the scattering vector '*s*', respectively ($s = (2/\lambda)\sin(\theta/2)$), where λ is the wavelength, and θ is the radial scattering angle. Inspection of this figure reveals that there is the presence of a 'shoulder' in all these plaques characteristic of microphase separation. PP-1.5W-PP displays a SAXS shoulder at ca. 0.0135 Å^{-1}, which translates into an average interdomain spacing of ~74 Å. The higher HS containing analogs in this series possess an increased interdomain spacing of approximately 115 ± 5 Å. It is also pointed out that the aforementioned interdomain spacings somewhat exceed the actual interdomain spacings due to the slit geometry utilized to obtain the SAXS results. The SAXS shoulders associated with PP-4.0W-PP and PP-6.0W-PP are also somewhat less sharp, possibly indicating a broader microdomain size distribution, which results due to the greater dispersity of HS lengths in these samples. The EP-Monol based counterpart materials displayed similar SAXS results and are not shown here for brevity.

Fig. 4 displays the SS glass transition (SS T_g) behavior of the pure monols and the trisegments which incorporate a single TDI unit, i.e. PP-TDI-PP and EP-TDI-EP, which have calculated molecular weights of 2174 g/mol. The SS T_g's, as noted from the inflexion point, are −74.0 and −75.6 °C for pure PP-Monol and EP-Monol, respectively. In comparison, by approximately doubling the molecular weight in PP-TDI-PP and EP-TDI-PP, the number of 'free ends' are approximately halved as compared to those in the pure monols, which raises the SS T_g's by ca. 7 °C. It is also pointed out, that PP-TDI-PP and EP-TDI-EP led to only low viscosity 'liquids', unlike the materials which possessed HS based on the reaction of TDI and water, which were solids, an example of which was provided earlier in Fig. 2. This observation also underlines the importance of the urea groups and their bidentate hydrogen bonding capabilities

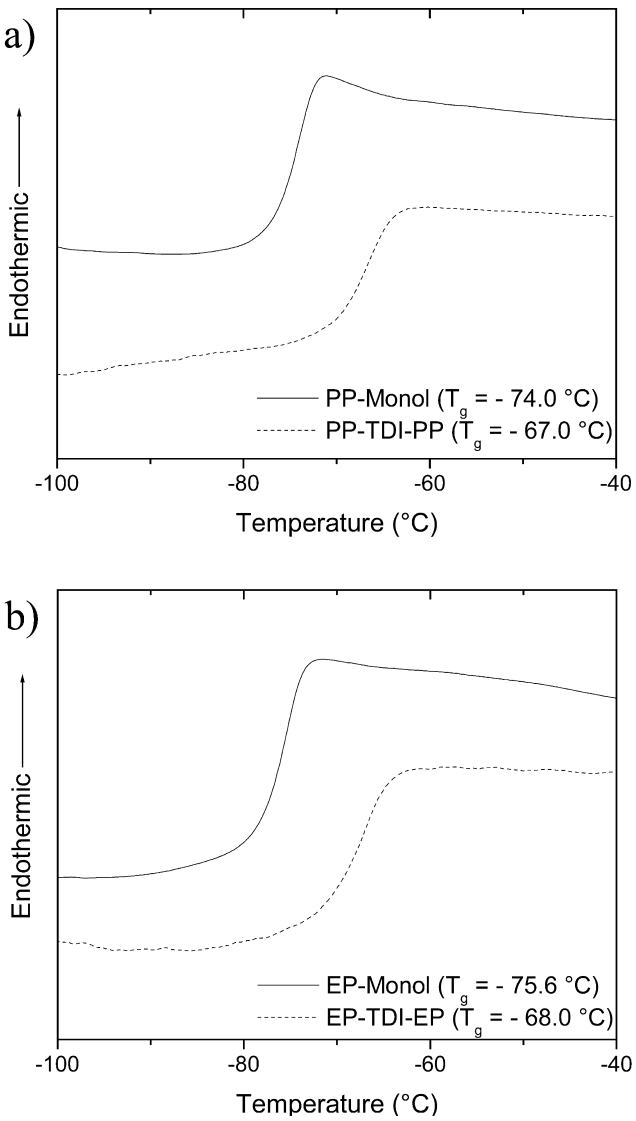

Fig. 4. Soft segment glass transition observed via DSC (a) PP-Monol and PP-TDI-PP, (b) EP-Monol, EP-TDI-EP.

which greatly enhance the association of the HS and change the state of a material from a liquid to a solid.

Fig. 5(a) and (b) display the DSC results obtained for the plaque samples based on PP-Monol and EP-Monol SS and containing HS based on the reaction of TDI and either 1.5, 2.0, 4.0, or 6.0 water pphp. As expected, the SS T_g values for these materials are higher (by ca. 10 °C) as compared to the pure monols on which they are based. However, the SS T_g values for these materials are merely 3 °C greater than PP-TDI-PP and EP-TDI-EP. This suggests that the SS T_g increases predominantly due to the loss of the free volume (associated with the free ends in PP-Monol and EP-Monol) which occurs when those free ends are reacted to form PP-TDI-PP and EP-TDI-EP. At this point, it is again strongly suggested that HS connectivity or percolation plays an important role in giving the plaques their cohesive strength and hence their solid state character. The lack of HS

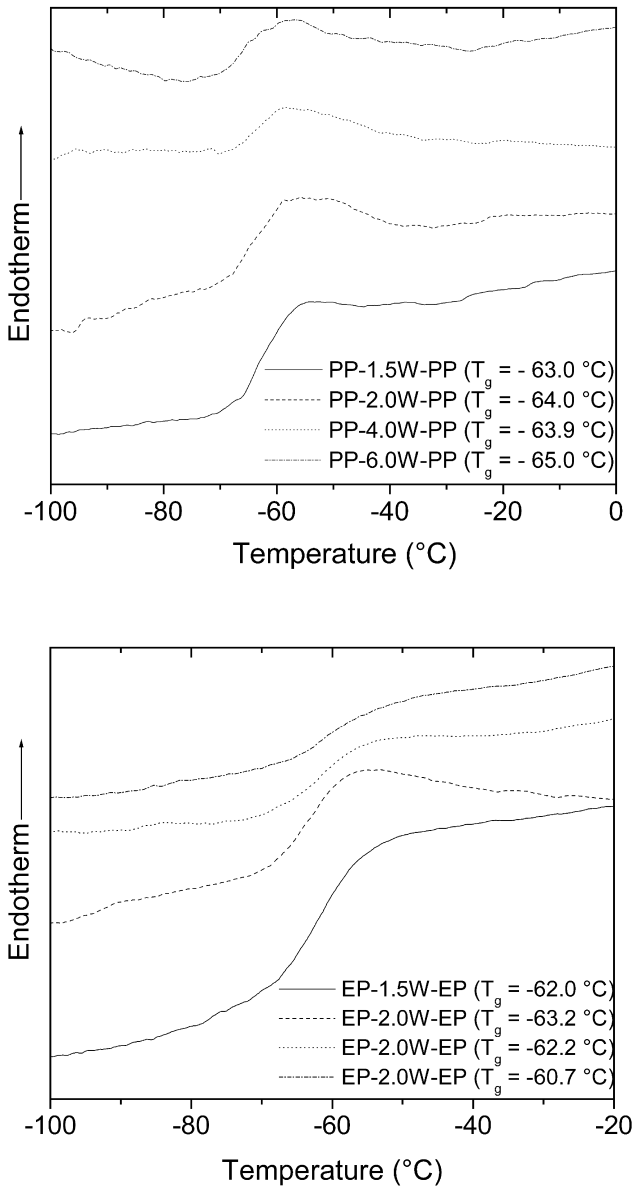

Fig. 5. Soft segment glass transition observed via DSC as a function of water (hard segment content) for plaques based on (a) PP-Monol soft segment, (b) EP-Monol soft segment.

connectivity in PP-TDI-PP and EP-TDI-EP maintains the liquid state of these materials.

Selected WAXS data are presented for the plaques in Figs. 6 and 7. It has been shown in several reports from this laboratory, that the HS based on 80:20 2,4/2,6 TDI and water are not crystalline but pack in a manner which leads to an observed d-spacing of ca. 4.7 Å [16–18,22]. This d-spacing has also been shown to correlate with a 1640 cm^{-1} FTIR absorbance which arises due to strong bidentate hydrogen bonding interactions between HS [22]. Also, it has been shown that due to differences in solubilization characteristics of the molded foam polyols (which contain higher EO repeating units) and slabstock foam polyols, the 4.7 Å is more distinct in slabstock systems [8]. This is also noted on comparing counterparts of Fig. 5(a) and (b), that the plaques based on PP-Monol display a distinctly sharper 4.7 Å reflection as compared to the EP-Monol based plaques. These figures also demonstrate that, as expected, increasing the HS content also intensifies the 4.7 Å reflection. The FTIR data for these samples, not presented for brevity, showed that the carbonyl region for the samples investigated in this study was characteristic of those observed for actual triol containing PU foams.

AFM is a widely used technique to examine phase separation in PU foams [16,17,22] and elastomers [23–25]. In tapping-mode AFM, which is one of the variations of AFM, 'phase' images can be obtained by detecting the phase shift between the actual oscillation of a tip and its drive oscillation. Conventionally, the scales of AFM phase images are set so that the harder phase induces a higher phase offset and appears lighter where as the softer phase appears darker. Therefore, in the AFM images presented in this paper, the lighter regions correspond the urea phase where as the softer regions are representative of the monol. The AFM images presented in this article are obtained by examining the free surfaces of the solution cast films or the films cast from the reacting mixture. It is also pointed out that there was no directional dependence observed in any AFM image as a result of casting films using a doctor blade.

AFM phase images for films cast from reacting mixtures are presented in Figs. 8–10. The AFM image of PP-1.0W-PP, presented in Fig. 8, shows that even at a HS content of 15.9 wt%, the microphase separated morphology is *not* composed of individual or isolated microdomains. Instead, the HS organize to form connected lath-like structures. Interestingly, percolation of the HS develops in these oligomeric systems at a lower HS fraction of 15.9% as compared to ca. 25% for the high molecular weight PU elastomers discussed earlier [14]. The onset of a percolated morphology in these systems at a relatively lower HS content is thought to be due to the relative ease of the low molecular weight chains to organize and assemble into interlocking domains. Fig. 9 displays the AFM image for PP-2.0W-PP, which contains 21.5 wt% HS. This image also shows *distinct* connectivity of the HS which helps explain the solid state of plaques. Further proof is provided in the AFM phase image of EP-2.0W-EP (Fig. 10), which shows the self-assembly of the urea HS to form continuous, percolated lath-like features. These features span several microns in the samples as was noted by collecting lower magnification images. It is also pointed out that reproducibility of this and the previous AFM images was checked by scanning different areas and also by using different tips. Connectivity of the HS was also noted in the higher water content samples (4.0 and 6.0 water pphp), but was difficult to distinctly resolve due to the higher volume fraction of the HS in these samples. Finally, AFM images from solution cast films, such as the one shown in Fig. 11, obtained from a redispersed solution cast film of sample EP-2.0W-EP, also shows the continuous nature of the hard phase which results

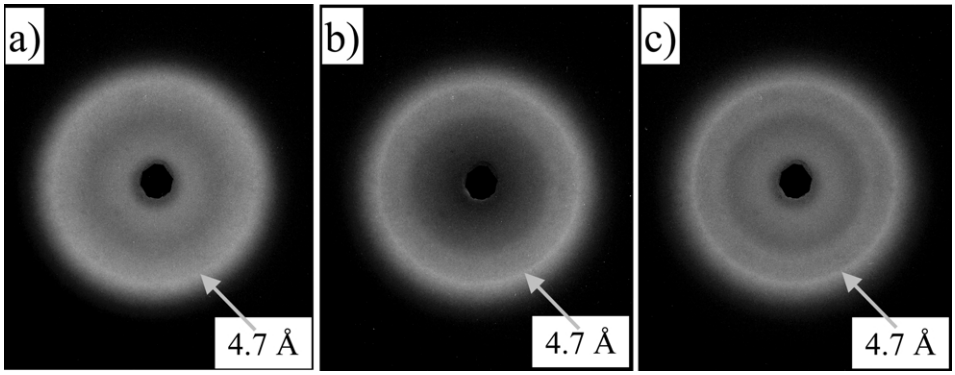

Fig. 6. Wide angle X-ray scattering patterns as a function of hard segment content (a) PP-2.0W-PP, (b) PP-4.0W-PP, and (c) PP-6.0W-PP.

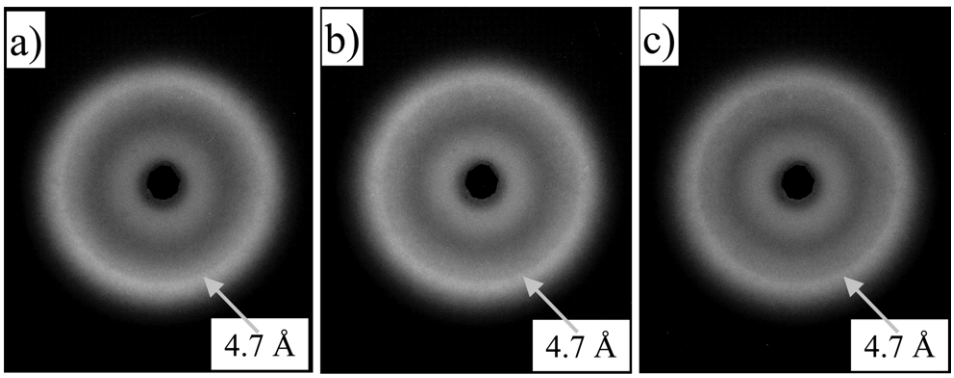

Fig. 7. Wide angle X-ray scattering patterns as a function of hard segment content (a) EP-2.0W-EP, (b) EP-4.0W-EP, and (c) EP-6.0W-EP.

due to of HS organization. This image is somewhat less distinct than the one presented in Fig. 10 and this may be due to the influence of the solvent on the precipitation of the urea phase. However, it is clear that the percolated HS texture is again generated upon film casting from solution.

While the microphase-separated morphology of the present monol systems may not be directly compared to that of actual triol containing PU foams, the present materials serve as 'model' systems to demonstrate the importance of HS connectivity in PU materials. Domain

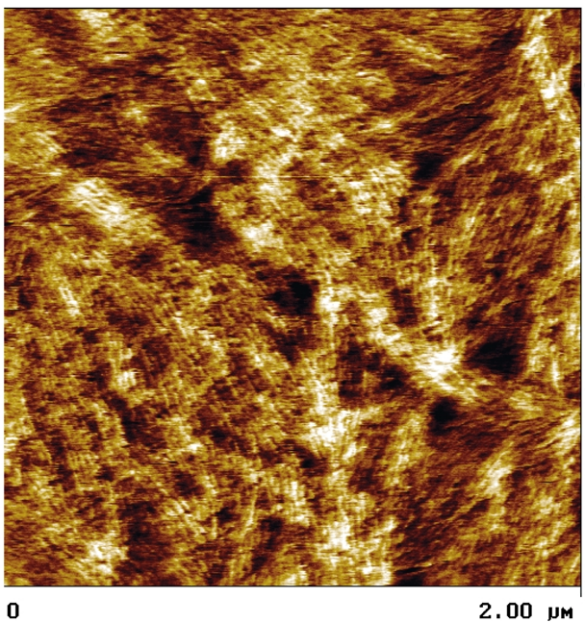

Fig. 8. $2 \times 2\ \mu m^2$ AFM phase image of surface of film PP-1.0W-PP cast from its reacting mixture.

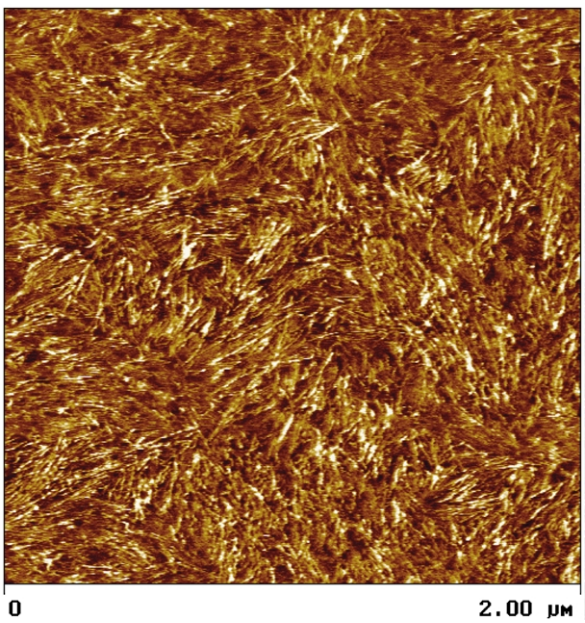

Fig. 9. $2 \times 2\ \mu m^2$ AFM phase image of surface of film PP-2.0W-PP cast from its reacting mixture.

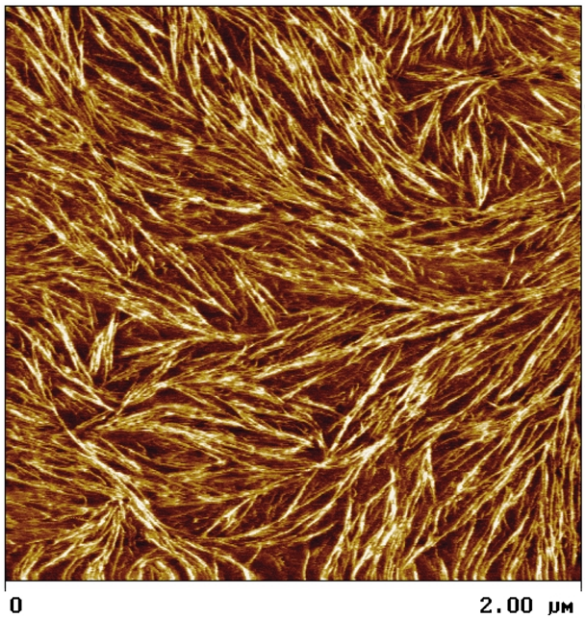

Fig. 10. $2 \times 2\ \mu m^2$ AFM phase image of surface of film EP-2.0W-EP cast from its reacting mixture.

sizes in flexible PU foams are thought to be of the order of 30–60 Å. However, researchers have often hypothesized, for example, by studying domain orientation behavior [26], that lamella-like features might be present in flexible PU foams. This study has, for the first time, allowed that connectivity of the hard phase may be promoted to the extent such that it changes the state of the material from a liquid to a solid state.

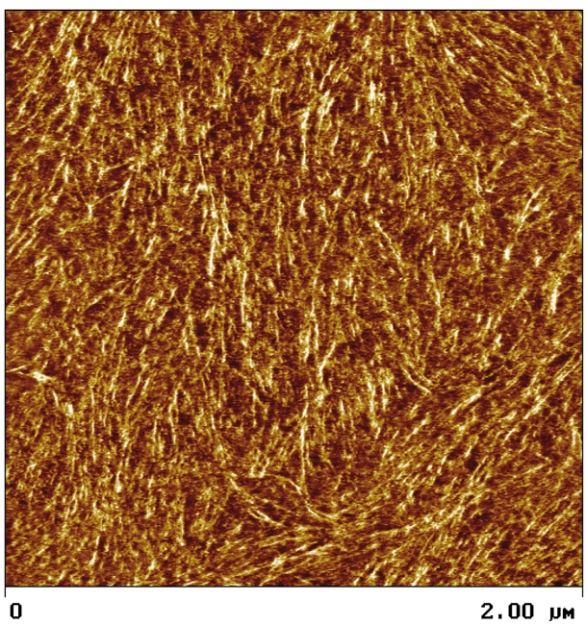

Fig. 11. $2 \times 2\ \mu m^2$ AFM phase image of solution cast film EP-2.0W-EP.

4. Conclusions

Model trisegmented PUs which are representative of flexible PU foams have been studied. The materials investigated employ TDI and water based HS, but utilize a monofunctional polyol (monol) as the SS, instead of the conventionally used triol in actual PU foams. SAXS, WAXS, DSC, and AFM were used to assess the microphase separated morphology of the materials. Plaques with HS contents varying from ca. 16 to 38 wt% are noted to be solid materials even at their low molecular weights of less than 3000 g/mol. Direct evidence which establishes the significance of HS connectivity in giving the plaques their solid-state has been provided via AFM. Furthermore, it is also shown that when the HS are not present (samples EP-TDI-EP and PP-TDI-PP), the materials remain in their liquid state.

Acknowledgements

The authors gratefully acknowledge Dow Chemical for financial support as well as for providing the materials and equipment at their facility in Freeport, Texas for the preparation of the samples used in this study. This material is based upon work supported in part by the US Army Research Laboratory and the US Army Research Office under contract/grant number DAAD19-02-1-0275 Macromolecular Architecture for Performance (MAP) MURI.

References

[1] Bayer O. Angew Chem 1947;59:257.
[2] Bayer O. Mod Plast 1947;24:149.
[3] Schollenberger CS, Scott H, Moore GR. Rubber World 1958;137:549.
[4] Schollenberger CS. US Patent 2,871,218 (01/27/59).
[5] Cooper SL, Tobolsky AV. J Appl Polym Sci 1966;10:1837.
[6] Hepburn C. Polyurethane elastomers, 2nd ed. London: Elsevier Applied Science; 1991.
[7] Chem Engng News, May 29, 2000; 78:42.
[8] Herrington R, Hock K. Flexible polyurethane foams, 2nd ed. Midland, MI: Dow Chemical Co.; 1998.
[9] Elwell MJ, Ryan AJ, Grunbauer HJM, Lieshout HCV. Macromolecules 1996;29:2960.
[10] Wilkes GL, Abouzahr S, Radovich D. J Cell Plast 1983;19:248.
[11] Armistead JP, Wilkes GL, Turner RB. J Appl Polym Sci 1988;35:601.
[12] Ade H, Smith AP, Cameron S, Cieslinski R, Mitchell G, Hsiao B, Rightor E. Polymer 1995;36:1843.
[13] Rightor EG, Urquhart SG, Hitchcock AP, Ade H, Smith AP, Mitchell GE, Priester RD, Aneja A, Appel G, Wilkes GL, Lidy WE. Macromolecules 2002;35:5873.
[14] Abouzahr S, Wilkes GL, Ophir Z. Polymer 1982;23:1077.
[15] Seymour RW, Cooper SL. Adv Urethane Sci 1974;3:66.
[16] Aneja A, Wilkes GL. J Appl Polym Sci 2002;85:2956.
[17] Aneja A, Wilkes GL. Polymer 2002;43:5551.
[18] Aneja A, Wilkes GL, Yurtsever E, Yilgor I. Polymer 2003;44:757.
[19] Aneja A, Wilkes GL, Yilgor I, Yilgor E, Yurtsever E. J Macromol Sci: Phys 2003; B42,1125.

[20] Elwell MJ, Ryan AJ, Grünbauer HJM, Van Lieshout HC. Macromolecules 1996;29:2960.
[21] Lin YC, Kachar B, Weiss RG. J Am Chem Soc 1989;111:5542.
[22] Kaushiva BD, McCartney SR, Rossmy GR, Wilkes GL. Polymer 2000;41:285.
[23] Garrett JT, Siedlecki CA, Runt J. Macromolecules 2001;34:7066.
[24] McLean RS, Sauer BB. Macromolecules 1997;30:8314.
[25] O'Sickey MJ, Lawrey BD. J Appl Polym Sci 2002;84:229.
[26] Kaushiva BD, Wilkes GL. Polym Commun 2000;41:6987.